

Experimental Results in Heavy Flavor Physics

Sheldon Stone

Department of Physics, Syracuse University, Syracuse, NY, USA, 13244-1130 e-mail: Stone@physics.syr.edu

Received: October 15, 2003

Abstract. The interplay of experiment and theory is explored in the context of current data on b and c decay. Measurements of $|V_{cb}|$ and $|V_{ub}|$ are extracted from existing data. Conservative estimates give $|V_{cb}| = (46.2 \pm 1.2_{exp} \pm 2.3_{thy}) \times 10^{-3}$ and $|V_{ub}| = (3.90 \pm 0.16_{exp} \pm 0.53_{thy}) \times 10^{-3}$. Using these values along with data on B_d , B_s mixing and CP violation in the K_L system, the allowed region of the CKM parameters ρ and η is derived. Tests of factorization in two-body hadronic B decays to one heavy and one light meson are shown and compared with modern theories which are also used to see if there is new physics in two-body B decays to light mesons. The two new narrow D_{sJ} states, discovered by BaBar and CLEO, respectively, are interpreted in light of the observation of these states in B decays by Belle.

PACS. 13.25.Hw Decays of bottom mesons – 13.20.Fc Decays of charmed mesons

1 Introduction

Our physics goals include discovering, or helping to interpret, New Physics found elsewhere using b and c decays. We already know that there must be New Physics because the Standard Model cannot explain the large observed Baryon Asymmetry in the Universe or Dark Matter [1]. We also need to measure Standard Model parameters, the “fundamental constants” revealed to us by studying Weak interactions. Furthermore, understanding the theory of strong interactions, QCD, is necessary to interpret our measurements.

A complete picture requires many studies including rare decays and CP Violation; the latter is covered by H. Yamamoto [2]. I will give an overview and cover rare decays, and show how they can uncover new physics. Interpreting fundamental quark decays requires theories or models than relate quarks to hadrons in which they live and die. I will discuss some relevant concerns. Theoretical issues are dealt with in more depth by T. Mannel [3]. Yamamoto also covers future experiments.

2 Lifetimes

Lifetimes (τ) set the width (Γ) scale since $\tau \cdot \Gamma = \hbar$. Lifetimes of b -flavored hadrons are shown in Fig. 1 as compiled by the B-lifetime working group [4]. Note that the ratio of B^+ to B^0 lifetimes is 1.073 ± 0.014 , a 5.2σ difference, while the Λ_b and b -baryon lifetimes are lower than the B^0 .

New charm lifetimes from FOCUS [5] are very precisely measured. See Fig. 2.

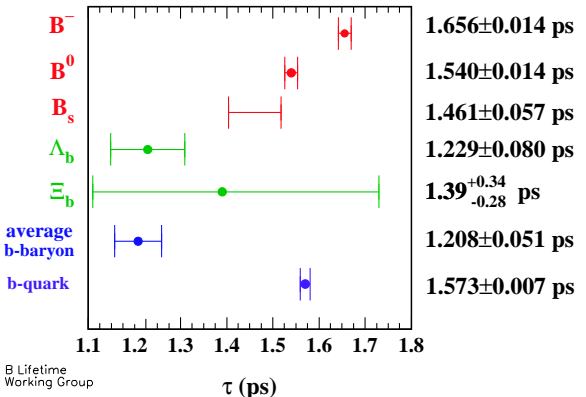


Fig. 1. Current measurement of lifetimes of b -flavored hadrons.

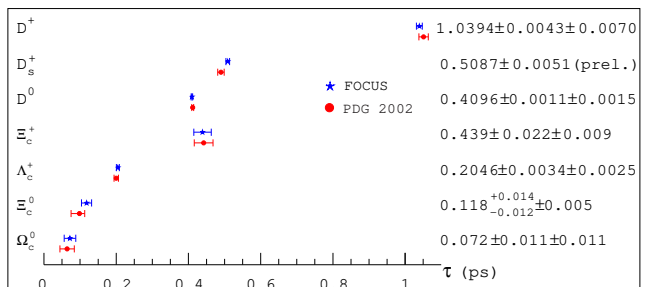


Fig. 2. New FOCUS measurement of charm lifetimes listed and compared on the plot with the PDG 2002 values.

3 The Basics: Quark Mixing and the CKM Matrix

The CKM matrix parameterizes the mixing between the mass eigenstates and weak eigenstates as couplings be-

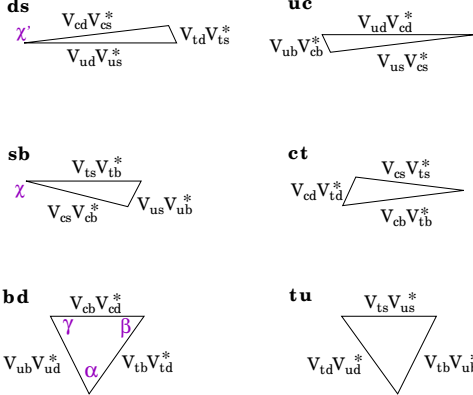


Fig. 3. The 6 CKM triangles resulting from applying unitarity constraints to the indicated row and column. The CP violating angles are also shown.

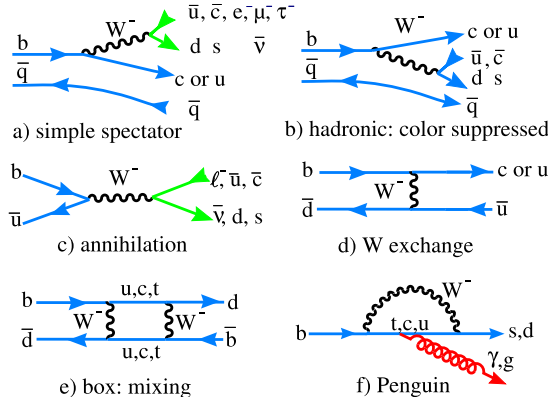


Fig. 4. Some B decay diagrams.

tween the charge $+2/3$ and $-1/3$ quarks. I use here the Wolfenstein approximation [6] good to order λ^3 in the real part and λ^4 in the imaginary part: $V_{CKM} =$

$$\begin{pmatrix} 1 - \lambda^2/2 & \lambda & A\lambda^3(\rho - i\eta)(1 - \lambda^2/2) \\ -\lambda & 1 - \lambda^2/2 - i\eta A^2 \lambda^4 & A\lambda^2(1 + i\eta \lambda^2) \\ A\lambda^3(1 - \rho - i\eta) & -A\lambda^2 & 1 \end{pmatrix}. \quad (1)$$

In the Standard Model A , λ , ρ and η are fundamental constants of nature like G , or α_{EM} ; η multiplies i and is responsible for all Standard Model CP violation. We know $\lambda=0.22$, $A \sim 0.8$ and we have constraints on ρ and η .

Applying unitarity constraints allows us to construct the six independent triangles shown in Fig. 3. Another basis for the CKM matrix are four angles labeled as χ , χ' and any two of α , β and γ since $\alpha + \beta + \gamma = \pi$ [7].

B meson decays can occur through various processes. Some decay diagrams are shown in Fig. 4. The simple spectator diagram is dominant. Semileptonic decays, which proceed through this diagram, are very useful and are discussed next.

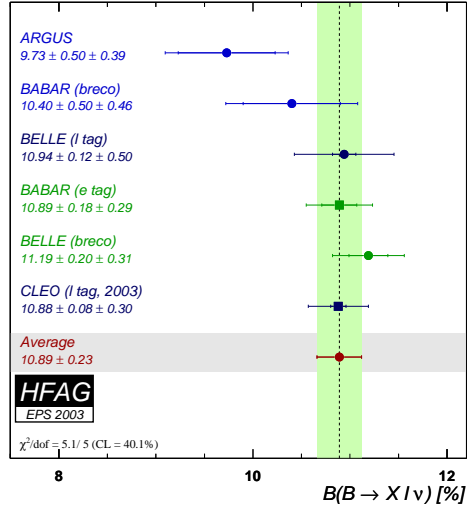


Fig. 5. B semileptonic branching ratio measurements from $\Upsilon(4S)$ decays.

4 The Semileptonic Branching Ratio

The total semileptonic branching of B mesons (\mathcal{B}_{sl}) can be measured using the process $\bar{B} \rightarrow X \ell^- \bar{\nu}$ in $\Upsilon(4S)$ decay, that contains an almost equal mixture of pair-produced charged and neutral B mesons. One problem arises because the decay sequence $B \rightarrow D \rightarrow Y \ell^+ \nu$ also produces leptons, albeit of lower momentum. The charge of these leptons, however, is opposite to those of the ones produced directly by the B decay. ARGUS long ago developed a technique of tagging the flavor of one B using a high momentum lepton. This allows the specification of the charge of the lepton directly from the second B in the pair. Corrections must be made for $B^0 - \bar{B}^0$ mixing and also leptons produced from D_s or D decays when they are produced by the virtual W^- as in Fig. 4(a). Fig. 5 shows the relevant measurements that result in $\mathcal{B}_{sl}=10.89 \pm 0.23\%$ [8].

LEP measurements average $10.59 \pm 0.22\%$. This number after correction for other b -species, by using the measured lifetimes, under the assumption that the semileptonic widths of all b species are equal, becomes $10.76 \pm 0.22\%$ for an average of B^0 and B^- , in excellent agreement with the $\Upsilon(4S)$ measurements.

5 Determination of $|V_{cb}|$ and $|V_{ub}|$

5.1 Introduction: Theory versus Models

Theories describe phenomena and make predictions based on general principles. They can have one or two unknown parameters (e.g. coupling constants) and if not exact, must prescribe a convergent series approximation. Some examples are Lattice QCD (unquenched) and Heavy Quark Effective Theory (HQET).

Models contain assumptions. It is not only that the models may be wrong that causes us a problem, just as serious is that the errors on the predictions are difficult to estimate.

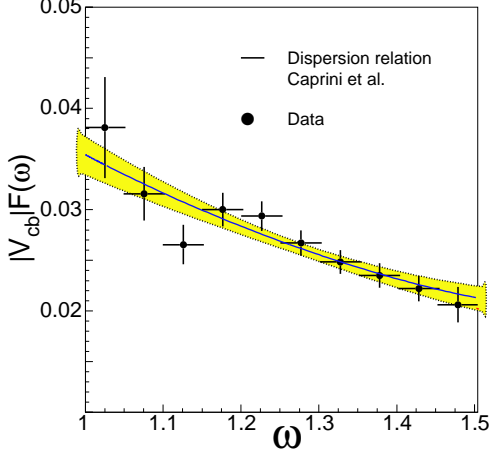


Fig. 6. Belle measurement of $F(\omega)|V_{cb}|$ using $\bar{B}^0 \rightarrow D^{*+} \ell^- \bar{\nu}$.

5.2 $|V_{cb}|$

5.2.1 Using Exclusive $B \rightarrow D^* \ell^- \bar{\nu}$ Decays

We are in the fortunate situation here of having a theory, Heavy Quark Effective Theory (HQET) formulated by M. Wise and the late N. Isgur [9]. This theory is based on the idea that QCD is flavor independent, so in the limit of infinitely heavy quarks the transition $q_a \rightarrow q_b$ occurs with unit form factor, ($F(1) = 1$) when the quarks are moving with the same invariant four-velocity, ω . Corrections to $F(1)$ for the fact that the b and c are not infinitely heavy are calculable in terms of a series, $\sum_n C_n (1/m_{i,j})^n$, where i and j refer to b and c , along with QCD corrections.

For determining $|V_{cb}|$ it is best to use the reaction $\bar{B} \rightarrow D^* \ell^- \bar{\nu}$, because it has a large branching rate and the $1/m_{i,j}$ corrections vanish [10]. Although, in principle there are three independent form-factors for this decay, due to the three possible D^* spin states, in HQET they are all related to one universal shape that can be measured. The idea is to determine the decay rate at ω of 1. Here the D^* is at rest in the B frame.

This measurement has been performed by several groups. Fig. 6 shows recent measurements from Belle for the reaction $\bar{B}^0 \rightarrow D^{*+} \ell^- \bar{\nu}$. To find the value for $F(1)|V_{cb}|$ the data are plotted as a function of ω and then fit to a shape function given by Caprini *et al.* [11]. The curvature of this function is denoted as ρ^2 and also is found in the fit. Data from other experiments is summarized in Fig. 7. All use the same reaction except CLEO which also uses $B^- \rightarrow D^{*0} \ell^- \bar{\nu}$.

The world average values given by the Heavy Flavor Averaging Group (HFAG) are $F(1)|V_{cb}| = (38 \pm 1.1) \times 10^{-3}$ and $\rho^2 = 1.49 \pm 0.15$ [8]. To find $|V_{cb}|$ we must evaluate $F(1)$, where $F(1) = \eta_{QED} \eta_{QCD} (1 + \delta_{1/m^2} + \dots)$. Current evaluations have $\eta_{QED} = 1.007$, $\eta_{QCD} = 0.960 \pm 0.007$ at the two loop level. The δ_{1/m^2} term evaluation has been summarized for the PDG by Artuso and Barberio [12] giving $F(1) = 0.91 \pm 0.05$; eventually unquenched Lattice Gauge calculations should be used. Thus we have

$$|V_{cb}| = (46.2 \pm 1.2_{exp} \pm 2.3_{thy}) \times 10^{-3} . \quad (2)$$

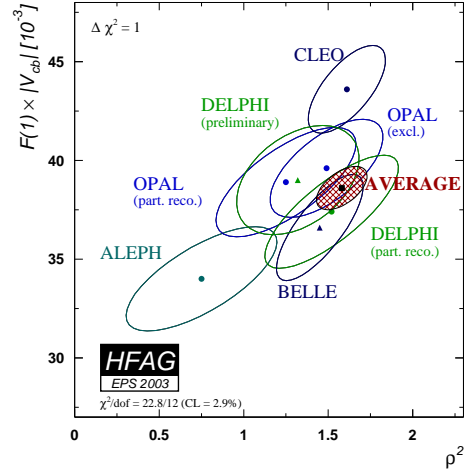


Fig. 7. Compilation of $F(1)|V_{cb}|$ versus ρ^2 measurements.

5.2.2 Using Inclusive Semileptonic Decays

The Heavy Quark Expansion (HQE) is a framework that allows predictions of the total widths, $b \rightarrow c$ or $b \rightarrow u$ semileptonic widths. It relies on $m_b \gg \Lambda_{QCD}$ and uses the Operator Product Expansion to express the decay widths in a double series in $1/m_q^n$ and α_s^n [13].

The HQE suffers from some serious problems. Terms of the order of $1/m_b^3$ are multiplied by unknown functions, that it make it difficult to evaluate the error at this order. Even more importantly, there is inherent assumption, called "Duality," having the meaning that integrated over enough phase space the physical finite exclusive charm bound states and the inclusive hadronic result will match at the quark level. However, there is no known way to evaluate the error due to this assumption.

Using the HQE, Bigi predicts that the Λ_b and b -baryon lifetimes will be no more than 10% lower than the B^0 lifetime [14]. However, τ_{Λ_b} and $\tau_{b\text{-baryon}}$ are lower by $20 \pm 5\%$ and $18 \pm 3\%$, respectively. It is possible, that that semileptonic widths are easier to predict than hadronic widths, so this failure does not necessarily make the HQE model useless, yet it does not add to our confidence in using it.

What is required is an experimental test in semileptonic decays, that can be used to evaluate the errors due to duality and the $1/m_b^3$ terms. Two tests are possible. One is to use the model in charm decays. This hasn't been done since m_c has been considered as too small, but it could be done to see how much the model diverged by measuring V_{cs} and V_{cd} . Another test is V_{cb} . Then we would have a pretty good measure of the uncertainties for V_{ub} .

The HQE expansion uses three experimental parameters to describe the decay rate to order $(\Lambda_{QCD}/m_b)^2$. First is the kinetic energy of the residual b -quark motion,

$$\lambda_1 = \frac{M_B}{2} \langle B(v) | h_v(iD)^2 h_v | B(v) \rangle . \quad (3)$$

The second parameter is the chromo-magnetic coupling of the b -quark spin to the gluon field, given by the measured

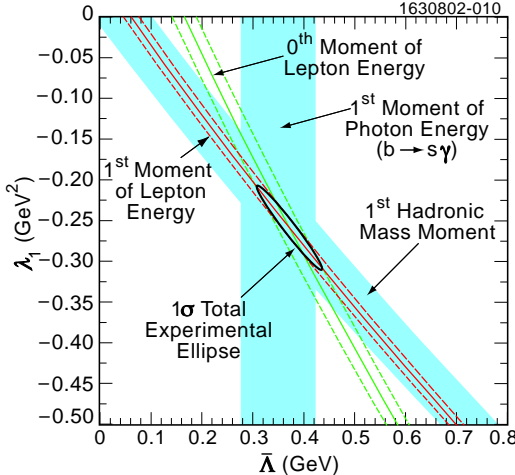


Fig. 8. Constraints on λ_1 versus $\bar{\Lambda}$ from CLEO hadronic and lepton energy moments and the first moment of the photon energy in $b \rightarrow s\gamma$.

$B^* - B$ splitting as 0.12 GeV^2 ,

$$\lambda_2 = -\frac{M_B}{2} \langle B(v) | h_v(g/2) \sigma^{\mu\nu} G_{\mu\nu} h_v | B(v) \rangle. \quad (4)$$

Finally the parameter $\bar{\Lambda}$ relates the meson and quark masses via

$$\begin{aligned} M_B &= m_b + \bar{\Lambda} - (\lambda_1 + 3\lambda_2)/(2m_b) \\ M_{B^*} &= m_b + \bar{\Lambda} - (\lambda_1 - \lambda_2)/(2m_b). \end{aligned} \quad (5)$$

Both λ_1 and $\bar{\Lambda}$ can be determined by measuring average quantities called “moments.” Useful terms in $b \rightarrow c\ell\bar{\nu}$ decays are the average mass of the charmed system decays, the zeroth and first moment of the lepton energy, and in $b \rightarrow s\gamma$ decays the first moment of the photon energy. The CLEO data are shown in Fig. 8 [15].

From these measurements CLEO extracts $|V_{cb}| = (40.8 \pm 0.5 \pm 0.4 \pm 0.9) \times 10^{-3}$, where the first error is due to the uncertainty on the total semileptonic width, the second error is due to the uncertainty on the determination of λ_1 and $\bar{\Lambda}$ and the third error reflects the theoretical uncertainty. A similar value was found by Bauer *et al.* using these and other data: $|V_{cb}| = (40.8 \pm 0.9) \times 10^{-3}$ [16]. A value within $\sim 7\%$ of the one found using $B \rightarrow D^* \ell\nu$.

Other groups have also done moments analyses. BaBar analyzes only the hadronic moments. Their results are listed in Table 1 [17]. Fig. 9 shows the first hadronic moment as a function of minimum lepton momentum for both old and updated BaBar and CLEO data. The data are in good agreement and consistent with theory.

BaBar has also combined other measurements of lepton and hadron moments separately and find the differences shown in Fig. 10. These differences could indicate a duality violation, but the data need to get better to establish that. Note that a difference of 0.2 GeV in m_b leads to a 20% change in V_{ub} using HQE. DELPHI have also presented a new analysis where they use m_b as an input which gives them some sensitivity to the $1/m_b^3$ terms [18]. To sum up, the situation is still evolving.

Table 1. Results of Moments Analyses

Group	$ V_{cb} \times 10^{-3}$	$m_b \text{ (GeV)}$
CLEO	$40.8 \pm 0.6 \pm 0.9$	$4.82 \pm 0.07 \pm 0.11$
BaBar	$42.1 \pm 1.0 \pm 0.7$	$4.64 \pm 0.09 \pm 0.09$
DELPHI	$42.4 \pm 0.6 \pm 0.9$	input

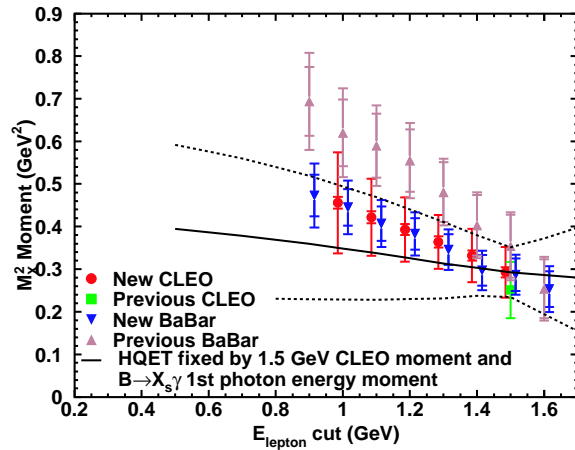


Fig. 9. First moment of the hadronic mass from BaBar and CLEO, both old and updated measurements.

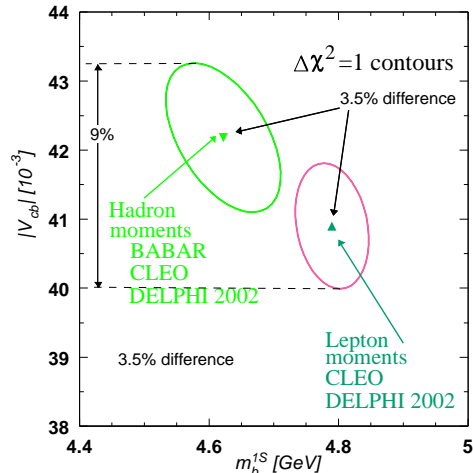


Fig. 10. Differences between hadron and lepton moments with experimental errors only.

5.3 $|V_{ub}|$

In this case there is no good theory. Modeling errors will dominate the experimental errors and our path through this discussion will be perilous.

5.3.1 Using Exclusive Semileptonic Decays

The decays $B \rightarrow \pi(\text{ or } \rho)\ell\nu$ can be used along with predictions from Lattice QCD. Fig. 11 show the predictions of three quenched Lattice QCD calculations for four-

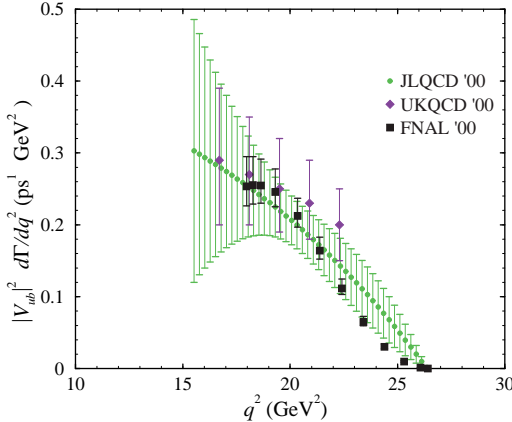


Fig. 11. Predictions of Lattice QCD for $B \rightarrow \pi \ell \nu$ from [19].

momentum transfer $q^2 > 16 \text{ GeV}^2$ from Kronfeld [19]; the error currently on these calculations is $\sim 10\%$ with an addition $\sim 20\%$ quenching error. There are also calculations over the entire q^2 range from other models, such as QCD sum rules [20].

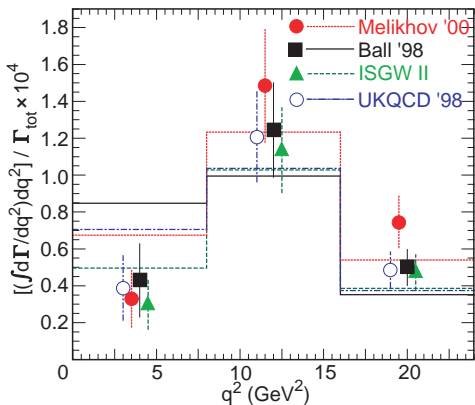


Fig. 12. CLEO measurements of the q^2 distribution for $B \rightarrow \rho \ell \nu$ compared with various models.

CLEO made the first measurements of $B \rightarrow \pi$ (or ρ) $\ell \nu$ decay rates and measured a rough q^2 distribution [21], that allows them to significantly reduce the systematic errors in their efficiencies (see Fig. 12). Using quenched Lattice results for $q^2 > 16 \text{ GeV}^2$ and light cone sum rules for smaller q^2 , they quote

$$|V_{ub}| = (3.17 \pm 0.17^{+0.16+0.53}_{-0.17-0.39} \pm 0.03) \times 10^{-3}, \quad (6)$$

where the errors are statistical, systematic, theoretical and $\rho \ell \nu$ form-factor, respectively.

BaBar has also measured $B \rightarrow \rho \ell \nu$. Averaging over one Lattice model and various form-factor models they quote

$$|V_{ub}| = (3.64 \pm 0.22 \pm 0.25^{+0.39}_{-0.56}) \times 10^{-3}, \quad (7)$$

with the same error sequence except without the last term [22]. The theoretical errors are assigned by each experiment. Are they large enough?

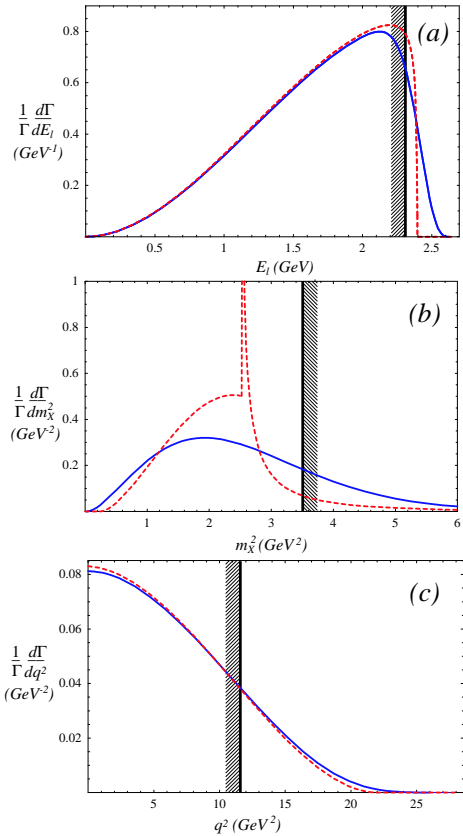


Fig. 13. The shapes of the lepton energy (a), hadronic mass (b) and leptonic mass (c) spectra. The dashed curves are for free b quark decay while the solid curves have the Fermi motion included in a model dependent manner. The unshaded side of the vertical bars correspond to regions used by experiments to suppress $b \rightarrow c$ background. (From Luke [23].)

5.3.2 Using Inclusive Semileptonic Decays

Using the HQE framework a theoretical accuracy of $\sim 9\%$ is obtainable if the entire $b \rightarrow u$ semileptonic decay rate was measured. The theoretical limitations are imposed by the accuracy on m_b of about 0.1 GeV (the decay rate goes as m_b^5) and the duality error which I limited to 7% based on $|V_{cb}|$. However, experimental cuts are required to reduce the ~ 100 times larger $b \rightarrow c$ rate and this usually means severely restricting the phase space. Unfortunately, as emphasized by Luke [23], these cuts exaggerate the theoretical errors. Fig. 13 show the parton model rates and the modification due to the Fermi motion of the b quark for a particular choice of spectral function $f(k^+)$. In general $f(k^+)$ is unknown, although knowledge about it can be derived in leading order only from the photon spectrum in $b \rightarrow s \gamma$.

Another pernicious consideration is that charged B mesons can have the b and \bar{u} quarks annihilate producing a lepton- $\bar{\nu}$ pair along with two gluons, thereby breaking the helicity suppression. The two gluons can turn into light hadrons. This is, in fact, a $b \rightarrow u$ process but not the one we want to consider because it supplements the $b \rightarrow u W^-$ rate, but is not accounted for by the theoretical

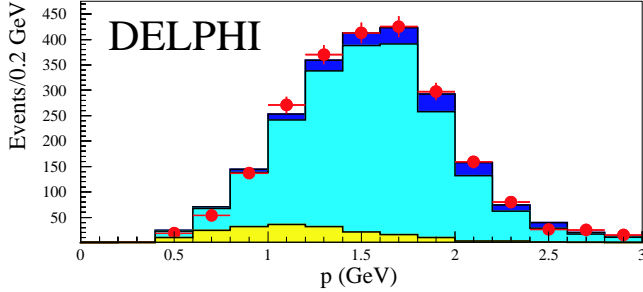


Fig. 14. The lepton momentum distribution in the B rest frame for $b \rightarrow u$ enriched decays. The data are the points, the dark shaded region the $b \rightarrow u\ell\nu$ signal, the medium shaded region the $b \rightarrow c\ell\nu$ background and the light shaded region other backgrounds.

calculations. Estimating this annihilation rate is difficult. A guess gives 3%. [24].

Luke has summarized the additional sources of errors arising from specific cuts restricting the signal phase space. The lepton energy cut (Fig. 13 (a)) is sensitive to $f(k^+)$ and sub-leading corrections, weak annihilation and may be more sensitive to duality because only $\sim 10\%$ of the $b \rightarrow u$ phase space is being used. The hadron mass cut (Fig. 13 (b)) is very sensitive to $f(k^+)$ and sub-leading corrections (see [25]). Making both q^2 and hadronic mass cuts is preferred if the minimum q^2 is as low as 7 GeV 2 , although there may be an increased sensitivity to m_b here [26].

Let us view the experimental results. ALEPH, DELPHI and L3 select samples of charm-poor semileptonic decays using a large number of selection criteria and performing a hadron mass cut < 1.6 GeV [27]. The DELPHI signal is shown as a function of lepton momentum in Fig. 14.

An average of all three measurements [28] gives the value

$$|V_{ub}| = (4.04^{+0.41+0.43+0.24}_{-0.46-0.48-0.25} \pm 0.19) \times 10^{-3}, \quad (8)$$

where the first error reflects statistical and detector systematics, the second from $b \rightarrow c$ modeling, the third $b \rightarrow u$ modeling and the fourth OPE uncertainties.

BaBar uses fully reconstructed hadronic B decays and then look for the semileptonic decay of the other B . They obtain an excellent signal to background of 2.5 to 1. Their sample of $b \rightarrow ul\nu$ events is plotted as a function of hadronic mass Fig. 15. Using the sample in the lowest bin, they quote

$$|V_{ub}| = (4.62 \pm 0.28 \pm 0.27 \pm 0.40 \pm 0.26) 10^{-3}, \quad (9)$$

where the errors are statistical, systematic, the fraction of $b \rightarrow u$ within their cuts and theory.

Next are the measurements using the end of the lepton momentum spectrum beyond where $B \rightarrow D\ell\nu$ can be produced. CLEO pioneered this technique and, in fact, it was the one used to first observe $b \rightarrow u$. The CLEO data is shown in Fig. 16. CLEO [29] and BaBar [30] report values

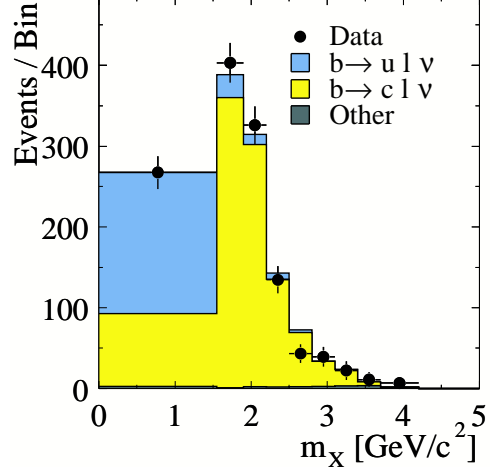


Fig. 15. The hadronic mass distribution from fully reconstructed tags from BaBar.

of

$$|V_{ub}| = (4.08 \pm 0.34 \pm 0.16 \pm 0.24) \times 10^{-3}, \quad (10)$$

$$|V_{ub}| = (4.43 \pm 0.29 \pm 0.25 \pm 0.35) \times 10^{-3},$$

respectively, where the errors are experimental, $b \rightarrow u$, OPE and $b \rightarrow s\gamma$. Belle also presented a preliminary value [31].

There are additional theoretical errors that, however, have not been assigned by the experiments. Bauer, Luke and Mannel point out that there is an additional uncertainty due to subleading twist contributions, basically higher order terms not accounted for using $b \rightarrow s\gamma$ for $f(k^+)$ [32]. Their estimate of the additional error caused by these terms is $\sim 15\%$. Furthermore, there is no assessment of the error due to weak annihilation which could be as large as 30%.

Belle has used two other techniques to measure $|V_{ub}|$. One uses $B \rightarrow D^{(*)}\ell\nu$ as a tag and the other uses neutrino reconstruction ala' exclusive semileptonic decays and then uses a sorting algorithm that they call "annealing" to separate the event into a tag side and a $b \rightarrow ul\nu$ side. To derive $|V_{ub}|$ in both cases they use $M_x < 1.5$ GeV and for the second they add a $q^2 > 7$ GeV 2 requirement [31]. Their values are

$$|V_{ub}| = (5.00 \pm 0.60 \pm 0.23 \pm 0.05 \pm 0.39 \pm 0.36) \times 10^{-3},$$

$$|V_{ub}| = (3.96 \pm 0.17 \pm 0.44 \pm 0.34 \pm 0.26 \pm 0.29) \times 10^{-3},$$

respectively, where the errors are statistical, systematic, $b \rightarrow c$, $b \rightarrow u$ and theoretical.

5.3.3 $|V_{ub}|$, Best Value and Error

A summary of all the measurements with the quoted errors added in quadrature is given in Fig. 17. We see that they are nicely clustered with an r.m.s. of $\sim 3 \times 10^{-2}$. However,

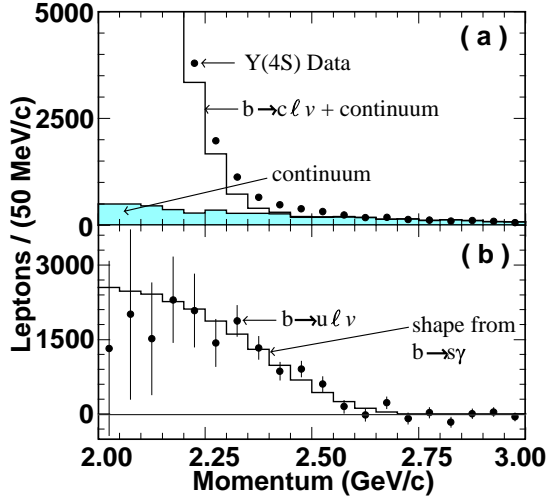


Fig. 16. The lepton momentum spectrum in the endpoint region from CLEO. (a) The data and (b) after continuum subtraction fit to a theoretical shape derived from the photon spectrum in $b \rightarrow s\gamma$.

it would be unwise to use this spread to assign an error for several reasons. First of all, there are theoretical errors that have not been included, and it seems that the more we learn about these decays the larger the errors become. Secondly, it is difficult to estimate how early measurements affected the central values of the ones that followed. Possibly it is safe to say that $|V_{ub}| = (4.0 \pm 1.0) \times 10^{-3}$. In the future there will be more data from the B factories with excellent tagging, such as demonstrated by the fully reconstructed tags from BaBar. Also, unquenched Lattice calculations for exclusive final states should become available in the large q^2 region.

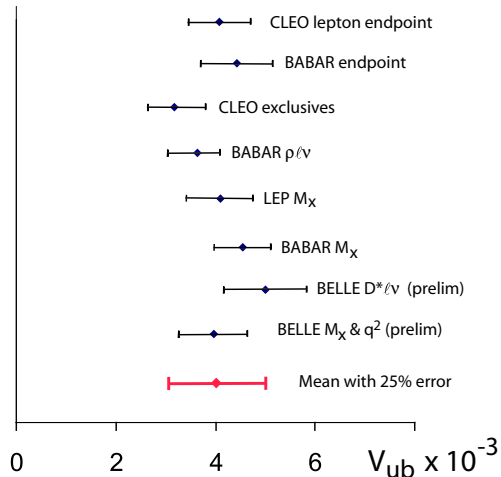


Fig. 17. Summary of $|V_{ub}|$ measurements.

I will now give a subjective evaluation of the current value of $|V_{ub}|$. Since we want to see if New Physics is present we need to be conservative in assigning errors. The

Table 2. Evaluation of $|V_{ub}|$. The first error is experimental and the second from theory.

Method	Experiment	$ V_{ub} (\times 10^{-3})$
Exclusives	CLEO & BaBar	$3.52 \pm 0.27 \pm 0.78$
Lepton endpoint	CLEO & BaBar	$4.28 \pm 0.27 \pm 1.44$
M_x cut	LEP & BaBar	Not used [25]
M_x & q^2 cuts	Belle	$3.96 \pm 0.47 \pm 0.56$
My Average		$3.90 \pm 0.16 \pm 0.53$

experimental statistical and systematic errors first need to be evaluated. For exclusive measurements I will use only quenched Lattice QCD calculations to turn the measured rate into a value for $|V_{ub}|$. These calculations have a 10% intrinsic error to which I add a 20% quenching error to arrive at a 22% total error. For inclusive measurements HQE is used and I add in the duality error, the error on m_b and the weak annihilation error, the sizes depending on the phase space region used by each measurement.

The values for the different methods are listed in Table 2. For exclusive final states I averaged CLEO and BaBar $\rho l \nu$ and CLEO $\pi l \nu$, using only Lattice QCD with a 22% error. For the lepton endpoint, the theoretical error is taken as the quadrature of 10%- $b \rightarrow u$, 3.7%- $b \rightarrow s\gamma$, 15%-higher twist, 30%-weak annihilation, 7%-duality, 5%- m_b . Measurements using only an $M_x < 1.5$ GeV are not used due to the parton model singularity close to the cut and the large resulting theoretical uncertainty. I do use the Belle ‘annealing’ result that has both the $M_x < 1.5$ GeV cut and the $q^2 > 7$ GeV², where the theoretical errors are 7%-duality, 7%-weak annihilation and 10%- m_b . The average value, that is subjective but justifiable, is

$$|V_{ub}| = (3.90 \pm 0.16_{exp} \pm 0.53_{th}) \times 10^{-3} . \quad (11)$$

6 $B - \bar{B}$ and $D - \bar{D}$ Mixing

6.1 B_d and B_s Mixing

Mixing in the B_d system is very well measured [33]. The relationship between the measurement and the CKM matrix elements is given by

$$x \equiv \frac{G_F^2}{6\pi^2} B_B f_B^2 m_B \tau_B |V_{tb}^* V_{td}|^2 m_t^2 F \left(\frac{m_t^2}{m_W^2} \right) \eta_{QCD}, \quad (12)$$

where η_{QCD} is ~ 0.8 and F is a known function. The parameters B_B and f_B are currently determined only theoretically. In principle f_B can be measured, but it is very difficult. Finding $\mathcal{B}(B^+ \rightarrow \tau^+ \nu)$ would measure the product $f_B |V_{ub}|$. The best limit is $< 4.1 \times 10^{-4}$ from BaBar [34] that gives $f_B < 390$ MeV.

B_s mixing is governed by a equation similar to Eq(12), with all quantities referring now to the B_s and the important change that V_{ts} appears rather than V_{td} . This causes the oscillation rate to be rather high and only a lower

limit of $\Delta m_s > 14.4 \text{ ps}^{-1}$ at 95% confidence level exists, compared with $\Delta m_d = 0.502 \pm 0.006 \text{ ps}^{-1}$ for B_d [35].

When B_s mixing is measured we will learn about

$$|V_{td}|^2/V_{ts}|^2 = [(1 - \rho)^2 + \eta^2] \propto f_{B_s} B_{B_s}^2 / f_{B_d} B_{B_d}^2 \equiv \zeta^2,$$

which gives a circle in the $\rho - \eta$ plane centered at (1,0). The theoretical ratio on the right hand side is far easier to calculate than the individual terms. Lattice QCD provides the best values for ζ . Wittig's summary gives $\zeta = 1.15 \pm 0.05^{+0.12}_{-0.00}$ [36], while a recent partially quenched calculation gives $1.14 \pm 0.03^{+0.13}_{-0.02}$ [37]. For fits used to find the values of ρ and η I will use $1.215 \pm 0.030 \pm 0.075$.

CDF is making progress analyzing B_s . They have found the decay $B_s \rightarrow D_s^+ \pi^-$. Fig. 18 shows their B_s candidate mass spectrum [38]. The wider peak at lower mass results from the decay $B_s \rightarrow D_s^{*+} \pi^-$. Here the decay $D_s^+ \rightarrow \phi \pi^+$ is used. CDF has measured the product of the ratio of production ratios and two-body B branching ratios as

$$\frac{f_s}{f_d} \cdot \frac{\mathcal{B}(\bar{B}_s \rightarrow D_s^+ \pi^-)}{\mathcal{B}(\bar{B}^0 \rightarrow D^+ \pi^-)} = 0.35 \pm 0.05 \pm 0.04 \pm 0.09. \quad (13)$$

Accumulating these events is needed to measure B_s mixing and CDF is off to a good start.

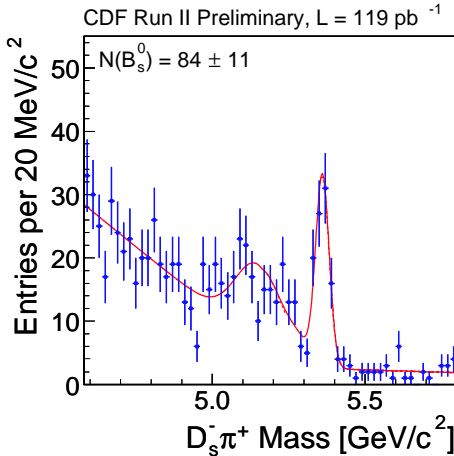


Fig. 18. The $D_s^+ \pi^-$ candidate mass spectrum for $D_s^+ \rightarrow \phi \pi^+$ from CDF. The curve is a fit to the signal shapes for $\bar{B}_s \rightarrow D_s^+ \pi^-$ (narrow peak) and $\bar{B}_s \rightarrow D_s^{*+} \pi^-$ (wide peak), where the γ from the D_s^{*+} decay is not observed. There are 84 ± 11 events in the narrow peak.

6.2 D^0 Mixing

Several groups have searched for, but not yet found mixing in the $D^0 - \bar{D}^0$ system. Measurements are made looking at the lifetime difference between CP equal to +1 and -1 eigenstates given by the parameter $y = \Delta\Gamma/2\Gamma$ and the mass difference between the two eigenstates given by the parameter $x = \Delta M/\Gamma$. Standard model predictions for these parameters are small, so this is a good place to look for the effects of new physics [39]. Alas, no evidence of

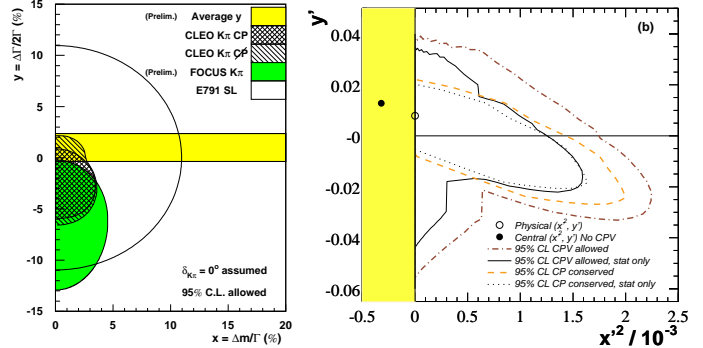


Fig. 19. Constraints on the size of $y = \Delta\Gamma/2\Gamma$ versus $x = \Delta M/\Gamma$ for both CP allowed and CP conserved scenarios from D^0 measurements. (a) Shows several experiments, while (b) is from BaBar only for $D^0 \rightarrow K^- \pi^+$. x' and y' refer to x and y allowing a rotation by an arbitrary phase.

such effects has been uncovered. Upper limits from several experiments are shown in Fig. 19 [40]. Analyses are done both not allowing CP violation in this system and also by permitting it.

7 Searches for New Physics: CKM Fits and Rare Decays

7.1 CKM Fits

There are many ways of looking for New Physics [41]. One interesting way to is use different kinds of measurements to determine the values of ρ and η [42]. We could in principle find ρ and η using only the magnitude measurements $|V_{ub}|$ and B mixing and see if different CP violating measurements give consistent values. We should separately test CP violation in K_L^0 decays, B_d decays (i.e. using $B^0 \rightarrow J/\psi K_s$ and $B^0 \rightarrow \rho\pi$) and B_s decays (i.e. using $B_s \rightarrow D_s K$ and $B_s \rightarrow J/\psi \eta$). Unfortunately we do not have these measurements at our disposal yet, though there are future dedicated hadron collider experiments, BTeV [43] and LHCb [44], that should provide them.

Several groups have performed fits to the CKM parameters and the methods are controversial. One set of groups, termed "Bayesians" treats the theoretical uncertainties as being Gaussian distributed [45]. Other groups eschew this prescription. They object because of the difficulties in assigning errors to models that have embedded assumptions. I use here the "Rfit" method. Theoretical errors are dealt with by restricting the theory variable to a 95% confidence interval with no preferred central value [46].¹ Fits for ρ and η using $|V_{ub}|$, B_d mixing, the upper limit on B_s mixing and CP violation in the kaon system ϵ_K give the result shown in Fig. 20. This is somewhat logically inconsistent since I am using ϵ_K , but this is what has been traditionally done. We then can compare with $\sin 2\beta$

¹ This group has kindly made their program available for use by others, see [47].

[2]. Treatment of the theoretical errors is particularly important here, as the theoretical errors are larger than the experimental ones for most of the input variables. Other non-Bayesian techniques give similar results as Rfit [48]; in particular, Dubois-Felsmann *et al.*, treat B_s mixing in a more conservative manner and find a somewhat larger region of acceptable values toward negative ρ .

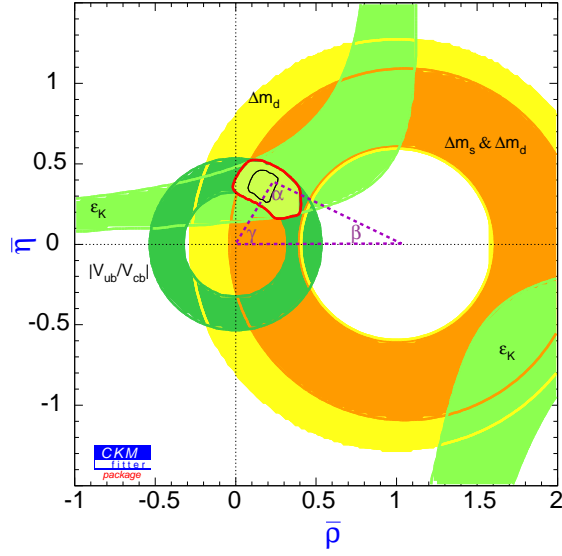


Fig. 20. Constraints on ρ and η using the value of the variables given in this talk for $|V_{ub}|/|V_{cb}|$ the upper limit on B_s mixing and B_d mixing, and ϵ_K from the PDG [33]. The outer circle is 95% c. l. and the inner one at 32%.

7.2 Rare b Decays

7.2.1 Rare Electromagnetic b Decays

Rare b decays are an excellent place to find new physics. Fig. 21 shows the basic structure of these processes. Heretofore unknown fermion-like objects can replace the quarks or new gauge-like objects can replace the W^- .

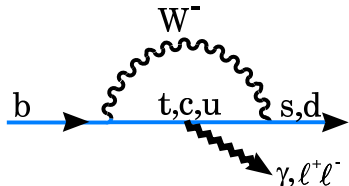


Fig. 21. Basic diagram for rare b decay.

Exclusive rare processes such as $B \rightarrow \rho\gamma$ and $B \rightarrow K^*\ell^+\ell^-$ are important as well as inclusive processes. For example Ali *et al.* show that SUSY can change the shape of the polarization in $K^*\ell^+\ell^-$ (see Fig 22) [49].

The inclusive rate for $b \rightarrow s\gamma$ is important in its own right and the shape of photon momentum spectra is used to get information on the Fermi momentum distribution

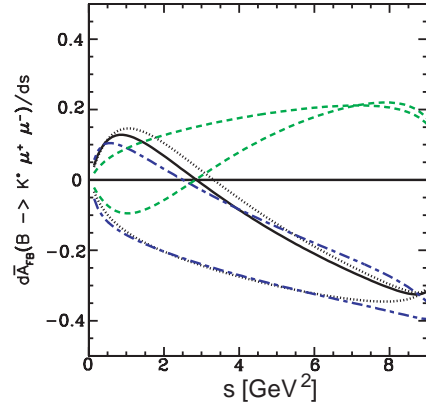


Fig. 22. Predicted dilepton asymmetry as a function of dilepton mass squared (s) for the Standard Model (solid line) and different SUSY models [49].

$f(k^+)$ of the b quark in the B meson, knowledge of which is needed for finding CKM matrix elements. CLEO still has the best determination [50].

$$\mathcal{B}(b \rightarrow s\gamma) = (3.21 \pm 0.43 \pm 0.27^{+0.18}_{-0.10}) \times 10^{-4}. \quad (14)$$

The continuum subtracted photon momentum distribution is shown in Fig. 23.

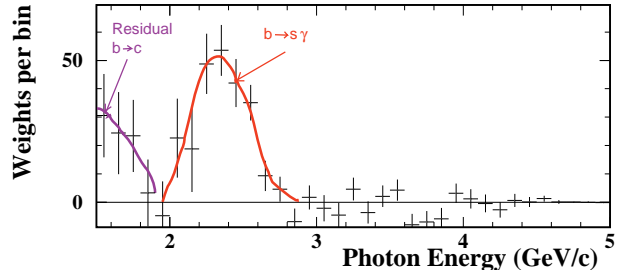


Fig. 23. Continuum subtracted photon momentum distribution for $b \rightarrow s\gamma$ from CLEO.

Other measurements have been made by ALEPH, Belle and BaBar [51]. The world average is

$$\mathcal{B}(b \rightarrow s\gamma) = (3.40 \pm 0.39) \times 10^{-4}. \quad (15)$$

In lowest order the Hamiltonian can be written as

$$\mathcal{H} = \frac{4G_F}{\sqrt{2}} (V_{tb}V_{ts}^*) [c_7(m_b)O_7 + c_8(m_b)O_8],$$

$$O_7 = \frac{e}{16\pi^2} m_b \bar{s}_L \sigma_{\mu\nu} b_R F^{\mu\nu}, \quad O_8 = \frac{1}{4\pi} m_b \bar{s}_L \sigma_{\mu\nu} b_R G^{\mu\nu}.$$

The resulting decay rate in the Standard Model is

$$\Gamma(b \rightarrow s\gamma) = \frac{G_F^2 \alpha m_b^5}{32\pi^4} |c_7|^2 |V_{tb}V_{ts}^*|^2. \quad (16)$$

Theorist then take $|V_{ts}| = |V_{cb}|$ and calculate the next to leading order (NLO) corrections. The full set of NNLO

Table 3. Branching ratios for rare dilepton decays ($\times 10^{-7}$).

Reaction	Belle	BaBar
$B \rightarrow K\ell^+\ell^-$	$4.8_{-0.9}^{+1.0} \pm 0.3 \pm 0.1$	$6.8_{-1.5}^{+1.7} \pm 0.4$
$B \rightarrow K^*\ell^+\ell^-$	$11.5_{-2.4}^{+2.6} \pm 0.8 \pm 0.2$	$14.0_{-4.9}^{+5.7} \pm 2.1$
$B \rightarrow X_s\ell^+\ell^-$	$61 \pm 14_{-11}^{+14}$	-

corrections has not yet been fully calculated. We are left with two predictions $(3.32 \pm 0.30) \times 10^{-4}$ and $(3.70 \pm 0.30) \times 10^{-4}$ (see Greub [52]), which I average to get a final SM theoretical prediction of $(3.5 \pm 0.5) \times 10^{-4}$, completely consistent with the data.

Many non-SM models are ruled out by this comparison. For example, Ali *et al.* define the parameters $R_i = (c_i^{SM} + c_i^{NP})/c_i^{SM}$, for $i = 7, 8$. Fig. 24 shows the contours allowed by the data along with the predictions of the SM and Supersymmetric Models with Minimal Flavor Violation [53].

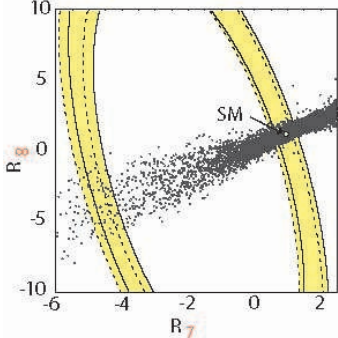


Fig. 24. Predictions of SM and MFV type SUSY models versus R_7 and R_8 (see text). The constraint from $b \rightarrow s\gamma$ is shown by the bands.

Belle first observed the dilepton decays in the $K\mu^+\mu^-$ final state [54]. Evidence for $K^*\mu^+\mu^-$ at the 3σ level was shown at this conference by BaBar [55]; recently Belle also has shown a signal in this mode [56]. Belle has also measured inclusive $X_s\ell^+\ell^-$ [57]. The branching ratios given in Table 3 are in agreement with SM predictions, but have large errors due to small statistics. For example, Belle has 30 $K^{*0}\ell^+\ell^-$ events in 140 fb^{-1} ; clearly much larger samples are needed to probe for new physics.

7.2.2 Rare Hadronic b Decays

First I will discuss some channels that do not proceed via loop diagrams. Let us consider phase shifts. In D decays the phase shifts are known to be large. In B decays CLEO [58] and Belle [59] observed $\bar{B}^0 \rightarrow D^0\pi^0$ which allowed the determination of the phase shift between the $\Delta I = 3/2$ and $\Delta I = 1/2$ amplitudes using the other two legs of the isospin triangle found from $\bar{B}^0 \rightarrow D^+\pi^-$ and $B^- \rightarrow D^0\pi^-$. The phase shift is found to be between 16.5° and 38.1° at 90% c. l. BaBar has also measured these decays [60].

Table 4. Factorization Tests.

Mode	$\bar{B}^0 \rightarrow D^{*+}\pi^-$	$\bar{B}^0 \rightarrow D^{*+}\rho^-$	$\bar{B}^0 \rightarrow D^{*+}a_1^-$
$\mathcal{B}(\%)$	0.28 ± 0.02	0.68 ± 0.09	1.30 ± 0.27
$d\Gamma/dq^2$	2.12	2.36	2.76
$(\text{ns}^{-1}\text{GeV}^{-2})$	$\pm 0.22 \pm 0.21$	$\pm 0.22 \pm 0.21$	$\pm 0.20 \pm 0.22$
f_h (MeV)	131.7	215	205
a_1	0.93 ± 0.07	0.85 ± 0.07	0.98 ± 0.11

Belle [61] and BaBar [62] have also observed the decay $\bar{B}^0 \rightarrow D_s^+ K^-$ at a level of 4×10^{-5} which can occur via the W exchange diagram shown on Fig. 25 or could be a result of rescattering from $D^+\pi^-$, for example. Phase shifts and rescattering go hand-in-hand.

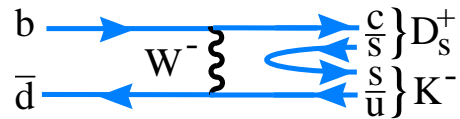


Fig. 25. W exchange diagram for $\bar{B}^0 \rightarrow D_s^+ K^-$.

We now consider the concept of “factorization.” This is a fundamentally simple idea, that the amplitude in two-body hadronic decays is a product of two hadronic currents similar to semileptonic decays (see Fig. 26) where there is one hadronic current and one leptonic current [65]. If factorization is a valid concept then the we can compare the decay widths for the hadronic two-body decay at q^2 equal to the mass-squared of the light hadron (h) according to the formula

$$\Gamma(\bar{B} \rightarrow D^* h^-) = 6\pi^2 a_1^2 f_h^2 |V_{ud}|^2 \frac{d\Gamma}{dq^2}(\bar{B} \rightarrow D^* \ell^- \bar{\nu}) \Big|_{q^2=m_h^2}, \quad (17)$$

where f_h is the decay constant for the light hadron and a_1 is a theoretical parameter. Early tests assumed that a_1 should be unity [66]. In BBNS, a modern theory of factorization, $a_1 = 1.05$ is a precisely calculated value [64].

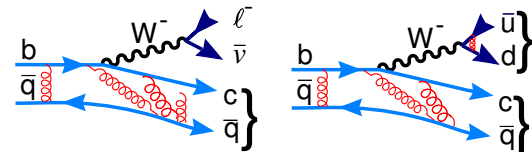


Fig. 26. Exclusive semileptonic decay and two-body hadronic decay into a $D^{(*)}$ plus light hadron. Gluons connecting the \bar{u} or d with the c or \bar{q} are ignored, hence factorization.

Table 4 compares available data on three hadronic modes with the semileptonic data from CLEO [67]. Unfortunately, other groups have not published their values of $d\Gamma/dq^2$.

The values of a_1 average about 14% below the BBNS predicted value. However, the CLEO value for $\mathcal{B}(\bar{B}^0 \rightarrow D^* \ell^- \bar{\nu})$ is 16% higher than the world average [8], implying that a_1 could be raised by 8% if other measurements of

Table 5. Branching ratios for $K\pi$ and $\pi\pi$ modes ($\times 10^{-7}$).

Mode	CLEO [69]	BaBar [70]	Belle [71]	Average
$\pi^+\pi^-$	45^{+14+5}_{-12-4}	$47\pm 6\pm 2$	$44\pm 6\pm 3$	45.5 ± 4.4
$\pi^+\pi^0$	46^{+18+6}_{-16-7}	$55^{+10}_{-9}\pm 6$	$53\pm 13\pm 5$	53 ± 8
$K^\pm\pi^\mp$	188^{+23+12}_{-21-9}	$179\pm 9\pm 7$	$185\pm 10\pm 7$	183 ± 7
$K^+\pi^0$	129^{+24+12}_{-22-11}	$128^{+12}_{-11}\pm 10$	$128\pm 14^{+14}_{-10}$	128 ± 11
$K^0\pi^-$	188^{+37+21}_{-33-18}	$200\pm 16\pm 10$	$220\pm 19\pm 11$	206 ± 13
$K^0\pi^0$	128^{+40+17}_{-33-14}	$104\pm 15\pm 8$	$126\pm 24\pm 14$	112 ± 14
$\pi^0\pi^0$	<47	$21\pm 6\pm 3$	$17\pm 6\pm 3$	19 ± 5

$d\Gamma/dq^2$ were available. Thus I conclude that the BBNS predicted value of a_1 is likely consistent with the data.

Now we turn to two-body rare decays into light hadrons. The leading diagrams are shown in Fig. 27. One is a simple spectator decay via $b \rightarrow u$ and the other is a loop decay. Since both diagrams can lead to the same final states, interference can occur.

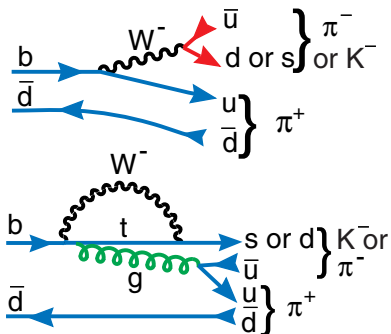


Fig. 27. Diagrams leading to charged $K\pi$ final states. (top) Decays via $b \rightarrow u$ and (bottom) Penguin decays.

These decays have been studied by several authors in a model dependent manner [63] and in the context of a QCD factorization theory by BBNS [64], who take the amplitude involving both the b and spectator quarks plus a part from the virtual W^- with corrections parameterized in a series $\propto \sum (4_{QCD}/m_b)^n$. They compute the amplitudes and the interferences for both the Tree and Penguin diagrams. Averaged experimental branching ratios are given in Table 5 [68].

The interference between the Tree ($\propto V_{ub}$) and the Penguin diagrams introduces the phase γ into the prediction of the decay rates. Discussing ratios rather than absolute rates reduces the errors. Some BBNS predictions are compared with the data from Table 5 in Fig. 28. We see that two of these ratios place restrictions of $80^\circ > \gamma > 58^\circ$, using 2σ as limiting the difference between the theory and data.

Certain other ratios present problems for this theory, however. The $K^0\pi^0/K^+\pi^0$ rate shown in the lower right hand corner, is relatively insensitive to γ , yet differs by more than 2σ from the prediction for $\gamma > 58^\circ$. BaBar and Belle recently observed $B^0 \rightarrow \pi^0\pi^0$ [72]. The prediction for $\tau_{B^+}/\tau_{B^0}\mathcal{B}(\pi^0\pi^0)/\mathcal{B}(\pi^\pm\pi^\mp)$ is < 0.12 for $\gamma < 80^\circ$ and < 0.27 for all γ . The measured ratio is 0.42 ± 0.11 , presenting another contradiction, although the $\pi^0\pi^0$ is particu-

larly difficult to predict because it is a low branching ratio color suppressed mode [74]. Since BBNS is a true theory, i. e. it makes predictions based on general principles and prescribes a convergent series approximation, then if future data do indeed continue to show inconsistencies with this theory the reasons for the theory breakdown must be understood. One possibility is that there is new physics present. A recent paper that approaches these decays in a different manner presents some evidence for new physics [73].

Ignoring these caveats, the allowed range $58^\circ > \gamma > 80^\circ$ is in excellent agreement with the allowed range of ρ versus η found by using the Rfit method, shown in Fig. 28. In fact this range is almost identical with the 32% confidence level allowed region outlined in the figure. Chua *et al.* have an alternative model that explicitly includes final state rescattering [75]. Using a similar set of reactions as BBNS, they find that γ is in the range of 90° - 100° , which is barely consistent with the values of ρ and η found by using Rfit, and more consistent with the range found by Dubois-Felsmann [48].

8 Revelations about QCD

Since QCD is so important for extracting quark parameters, it is interesting to see how well its doing in other areas. These include new narrow excited D_s states, doubly charmed baryons [76], measurements of the $\eta(2C)$ mass [77], D states in the Upsilon system [78] and D^{**} states in B decays [79]. Unfortunately, space allows only a discussion of one of these interesting topics.

8.1 The Narrow Excited D_s States

Excited D_s mesons have unit angular momentum between the c and \bar{s} quarks. Different couplings to the quark spin give predicted spin-parity, J^P , of: 0^+ , 1^+ , 1^+ and 2^+ . One 1^+ and the 2^+ have previously been seen. These decay into $D^{(*)}K$, and are relatively narrow. Other states were also predicted by most potential models to be above $D^{(*)}K$ threshold and have large ~ 200 MeV widths [80].

BaBar observes a “narrow” peak in the $D_s^+\pi^0$ mass distribution, shown in Fig. 29 [81]. The mass is $2316.8 \pm 0.4 \pm 3.0$ MeV, where the first error is statistical and the second systematic. The width is consistent with the mass resolution of ~ 9 MeV (r.m.s.). The mass is lighter than most potential model predictions and is 40 MeV below DK threshold.

Most potential models predicted the mass of this state to be above DK threshold. Those authors who did predict lower masses, did not point out that the state would be narrow (see for example [82], [83]). After the announcement of this discovery several possible explanations appeared, some of which were quite exotic. Barnes *et al.* argued the possibility of a DK molecule [84], while Szczepaniak argued for a $D\pi$ atom [85]. Van Beveren and Rupp use a unitarized meson model to explain the narrow mass as a kind of threshold effect [86]. Cahn and Jackson formulate an acknowledgement poor explanation using non-relativistic

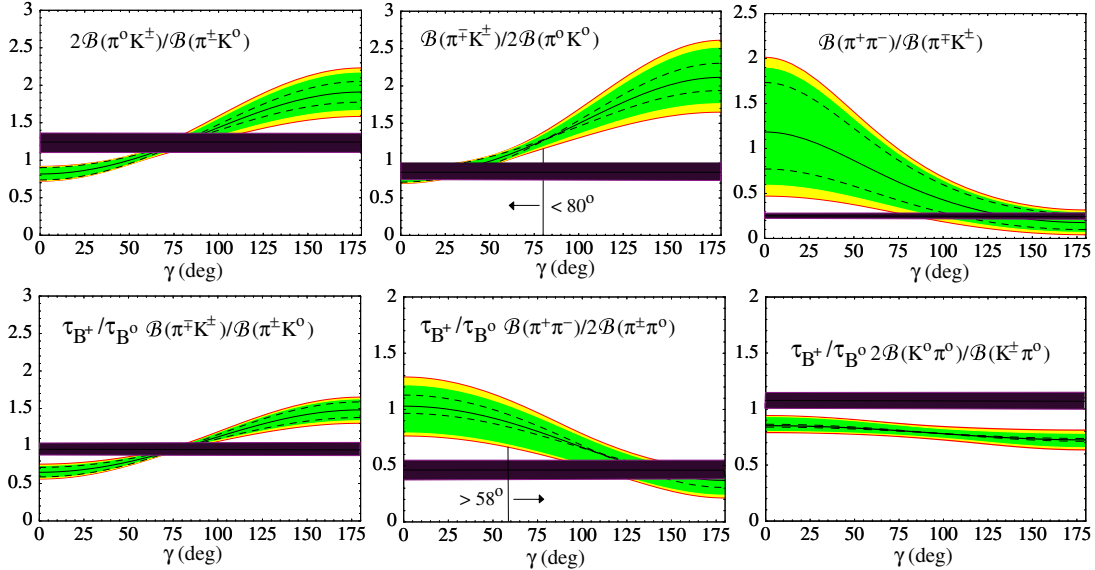


Fig. 28. Predictions from BBNS shown as curved bands and the world average data shown as horizontal bands (central value $\pm 1\sigma$) as a function of γ . The vertical bands on the center two plots indicate the values of γ where the measurements differ by 2σ from the edges of the theory bands.

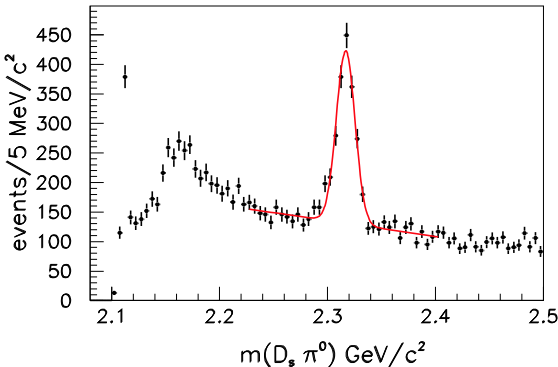


Fig. 29. The $D_s^+ \pi^0$ mass distribution from BaBar. The very narrow peak near threshold is from the isospin violating decay $D_s^{*+} \rightarrow \pi^0 D_s$.

vector and scalar exchange forces [87]. Several authors propose a four-quark explanation [88]. Bardeen, Eichten and Hill [89] explain the 2317 MeV object as an “ordinary” $c\bar{s}$ state, that is narrow only because isospin is violated in the decay.² The isospin violating channel is the only way for this state to decay since the mass is below DK threshold [90]. They use HQET plus chiral symmetry to predict “parity doubling,” where two orthogonal linear combinations of mesons transform as $SU(3)_L \times SU(3)_R$ and split into $(0^-, 1^-)$, $(0^+, 1^+)$ doublets. Assuming that the $D_{sJ}^*(2317)$ is the 0^+ state expected in the quark model, they predict that the mass splitting between the remaining 1^+ state and the 1^- should be the same as the $0^+ - 0^-$ splitting (see also [91]).

CLEO confirms the $D_s^+ \pi^0$ state seen by BaBar. They find, that the measured width of the peak is $8.0^{+1.3}_{-1.2}$ MeV,

² Isospin is violated because the D_s^+ and its excitations are $I=0$, while the pion is $I=1$.

somewhat wider than the detector resolution of 6.0 ± 0.3 MeV [92]. More interestingly, they also show unequivocal evidence of a second state decaying into $D_s^{*+} \pi^0$ at a mass near 2460 MeV (see Fig. 30). The measured width is 6.1 ± 1.0 MeV, close to the detector resolution of 6.6 ± 0.5 MeV. There are 55 ± 10 events in the peak. Although the BaBar data also showed an excess of events in this mass region, the conclusion reached in Ref. [81] was that further study was needed to resolve whether the peak received contributions from a new state or was entirely due to a reflection of the $D_{sJ}^*(2317)$. I will consider the questions of reflections and backgrounds next.

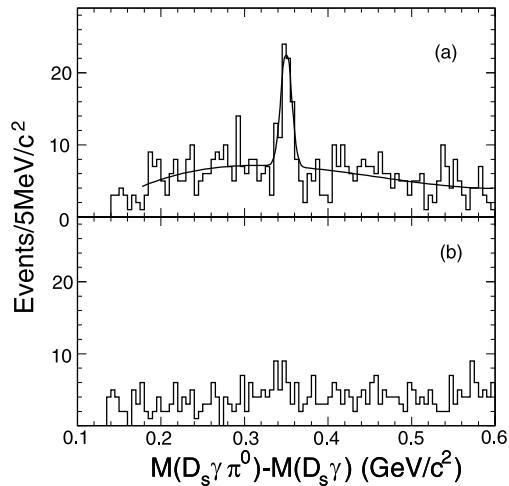


Fig. 30. The $D_s^{*+} \pi^0$ candidate mass distribution from CLEO shown as the difference with respect to the D_s^{*+} mass. (a) D_s^{*+} signal region; (b) D_s^{*+} sideband region.

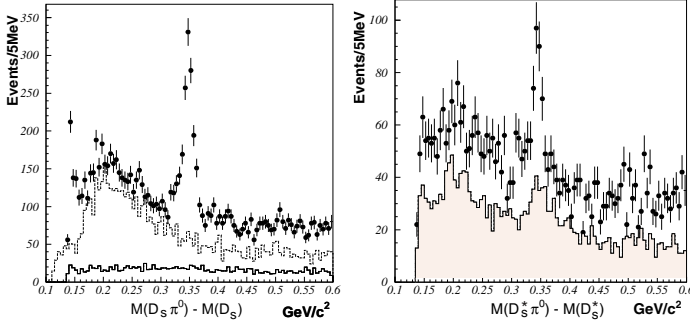


Fig. 31. Mass difference distributions from Belle. The histograms are (left) D_s^+ sidebands (dark dotted line) and π^0 sidebands (light dotted line) and (right) D_s^{*+} sidebands.

No known source has been identified that can create these narrow peaks, other than new resonances. However, in both cases the mass differences between the excited states and the D_s or D_s^* are about 350 MeV. This makes it easy for one state to reflect into another. The real question is how much of each observed peak is a reflection of the the other state. CLEO has two methods. In their first method they perform a Monte Carlo simulation of feed-down and feed-up. It turns out that the efficiency for the higher mass peak to appear near the lower mass peak by simply ignoring the photon from the D_s^* decay is quite high, $(84 \pm 4 \pm 10)\%$, but the predicted width of the peak is 14.9 MeV, rather larger than the observed width. By comparison, the feed-up is rather small, $(9.0 \pm 0.7 \pm 1.5)\%$ of the real signal in the lower mass peak, because a random photon must be picked up to form a D_s^* . The smallness of this feed-up is confirmed by small peaking in the D_s^* sidebands, Fig. 30(b), which represents about 20% of the total number of events in the signal peak.

In their second method CLEO fits the peak near 2317 MeV to two Gaussians, one from the feed-down and one for the narrow state; for the 2460 MeV state they perform a D^{*+} sideband subtraction before they fit the signal peak. In the 2317 MeV region, their fit determines the signal to be at a mean mass difference of $350.0 \pm 1.2 \pm 1.0$ MeV with a width of 5.9 ± 1.2 MeV and another wider Gaussian at 344.9 ± 6.1 MeV with a width of 16.5 ± 6.3 MeV, characteristic of the feed-down background. The systematic error on the mass of 1.0 MeV is smaller than the 3.0 MeV assigned by BaBar because CLEO has removed the effects of the feed-down background on the mass determination. The sideband subtracted fit in the 2460 MeV region gives a mass difference of $351.2 \pm 1.7 \pm 1.0$ MeV.

Belle confirms both peaks in continuum e^+e^- collisions [93]. The Belle data are shown in Fig. 31. There is clear peaking in the D_s^{*+} sideband region showing the level of feed-up. Furthermore, BaBar also now confirms the existence of the $D_s^{*+}\pi^0$ state [94].

Thus, there is no question about the existence of such states; we do need still to investigate what they are and what they tell us about QCD. CDF [95] and CLEO have looked for similar neutrally charged states in $D_s^\pm\pi^\mp$ and doubly charged states in $D_s^\pm\pi^\pm$. No signals were found.

The CLEO data is shown in Fig. 32; upper limits over the shown mass difference range are better than a factor of ten lower than the observed $D_s^+\pi^0$ signal [96]. CLEO also finds upper limits on many other decay channels of both states. The lack of any isospin partner states casts doubt on any molecular explanation.

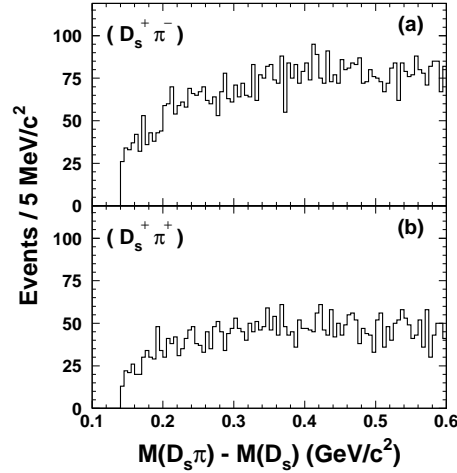


Fig. 32. (Mass difference distributions from CLEO for (a) $D_s^\pm\pi^\mp$ and (b) $D_s^\pm\pi^\pm$.

These states should also be seen in B decays. The modes $B \rightarrow D^{(*)}D_s^{(*)-}$ have been observed long ago [33]. Lipkin, in fact, predicted that the 1^+ states would be produced in the reaction $B \rightarrow DD_{sJ}^{(*)-}$ [97]. The diagram for such processes is shown in Fig. 33. Belle has observed these reactions [98]. Fig. 34 shows the reconstructed $D_s^+\pi^0$, $D_s^{*+}\pi^0$ and $D_s^+\gamma$ mass spectrum for events whose mass and beam energy constraints are consistent with the reaction $B \rightarrow DD_{sJ}^{(*)-}$.

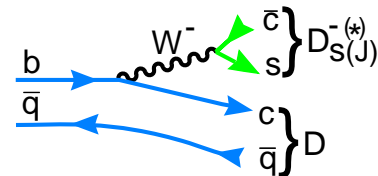


Fig. 33. Feynman diagram for $B \rightarrow DD_{sJ}^{(*)-}$.

The peak in Fig. 34(c) represents the first observation of the radiative decay mode of the $D_{sJ}(2460)$. The product branching ratios are given in Table 6.

The relative width of the radiative to the isospin violating decay is

$$\frac{\Gamma(D_{sJ}(2460) \rightarrow D_s\gamma)}{\Gamma(D_{sJ}(2460) \rightarrow D_s\pi^0)} = 0.38 \pm 0.11 \pm 0.04 \quad (18)$$

Another determination in the continuum by Belle, gives a somewhat inconsistent value of $0.63 \pm 0.15 \pm 0.15$ [99], the average value is 0.44 ± 0.10 .

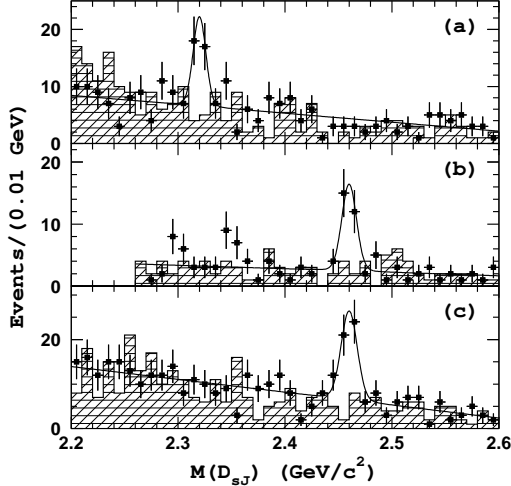


Fig. 34. Invariant masses for $D_{sJ}^{(*)-}$ candidates produced in the reaction $B \rightarrow DD_{sJ}^{(*)-}$. The open regions are signal, the cross hatched regions combinations of $D_{sJ}^{(*)}$ mass and ΔE sidebands for (a) $D_s \pi^0$, (b) $D_s^* \pi^0$ and (c) $D_s \gamma$.

Table 6. $\mathcal{B}(B \rightarrow DD_{sJ}^{(*)})$ from Belle

B mode	D_{sJ} mode	$\mathcal{B} \times 10^{-4}$
$DD_{sJ}^{*-}(2317)$	$\pi^0 D_s$	$8.5^{+2.5}_{-1.9} \pm 2.6$
$DD_{sJ}^-(2460)$	$\pi^0 D_s$	$17.8^{+4.5}_{-3.9} \pm 5.3$
$DD_{sJ}^-(2460)$	γD_s	$6.7^{+1.3}_{-1.2} \pm 2.0$

The branching ratio of $B \rightarrow DD_s^{(*)+}$ is $\sim 1\%$ [33]. Assuming that the decay modes shown in Table 6 are dominant, then the branching ratios to these excited states are about a factor of 4-10 lower. Chen and Li [100] and Cheng and Hou [88] predict that a four-quark state would have one order of magnitude lower branching ratio. Datta and O'Donnell agree that factorization predicts a similar rate for the excited states as the D_s^+ and show that a molecular explanation is consistent with the data [101]. Fundamentally, the disagreement with factorization arises out of assuming that the decay constant of these excited states is the same as that of the D_s^+ ; then taking either a molecular or four-quark structure for the new states allows the coupling to the virtual W^- to be smaller and thus explains the data.

The spin-parity, J^P , of these states can be inferred from their decay modes. Since the $D_{sJ}^{*+}(2317)$ decays into two pseudoscalars it is likely to be a 0^+ state, though higher spin cannot be ruled out. Similar reasoning would assign the $D_{sJ}^+(2460)$ as a 1^+ state. These assignments are strengthened by the non-observation of the radiative γD_s transition for the $D_{sJ}^{*+}(2317)$ and its observation for the $D_{sJ}^+(2460)$. Belle has confirmed the assignment for the $D_{sJ}^+(2460)$ by measuring the angular distribution in the B decay channel, shown in Fig. 35.

Fig. 36 summarizes the measurements of the mass difference between the $D_{sJ}^{*+}(2317)$ and the D_s^+ . The measurements are in good agreement. The world average mass

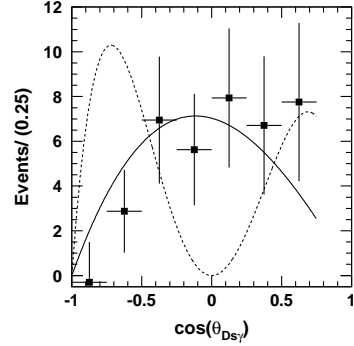


Fig. 35. Angular distribution in the reaction $B \rightarrow DD_{sJ}^-(2460)$, $D_{sJ} \rightarrow \gamma D_s^-$ of the D_s in the D_{sJ} rest-frame with respect to the D_{sJ} direction in the B rest-frame. The points with error bars are the data, the solid (dashed) curve the expectation for a 1^+ (2^+) D_{sJ} state.

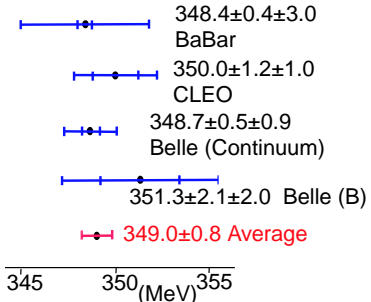


Fig. 36. Measurements of the mass difference between the $D_{sJ}^{*+}(2317)$ and the D_s^+ .

difference is 349 ± 0.8 MeV. Adding the PDG value for the D_s^+ mass of 1968.5 ± 0.6 MeV, we arrive at a mass of 2317.5 ± 1.0 MeV [33].

Fig. 37 summarizes the different measurements of the mass difference for the $D_{sJ}^+(2460)$. The CLEO measurement is somewhat larger than the Belle and BaBar continuum values but within error. Ultimately mass values using B reconstruction may be the best way to obtain mass values (for both states) as the feed across corrections are absent. The world average mass difference is 346.9 ± 1.2 MeV. Adding the PDG value for the D_s^+ mass of 2112.4 ± 0.7 MeV, we arrive at a mass of 2459.3 ± 1.4 MeV [33]. The mass splittings between the chiral doublets (spin-0 minus spin-1) is 2.1 ± 1.4 MeV, consistent with zero. This agrees with the “parity doubling” predictions using chiral symmetry coupled with HQET [89] [91].

CLEO limits the width $\Gamma < 7$ MeV for both states, experimentally, although predictions of widths in the quark model are at the level of ten keV [89] [102] [103].

Several calculations of the masses of these two narrow states give close to the correct values. These include quenched lattice [104], although an earlier lattice result did not agree [105], the MIT bag model [106] and QCD sum rules using HQET [107]. There continues to be some disagreement, however [108].

Most properties of these states can be explained if these particles are $c\bar{s}$ states. The chiral mass splittings,

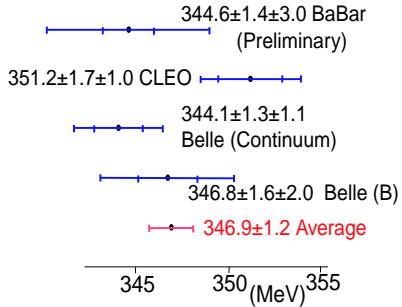


Fig. 37. Measurements of the mass difference between the $D_{sJ}^+(2460)$ and the D_s^{*+} .

between the 0^+ and 0^- are equal within experimental error to that between the 1^+ and 1^- , as predicted by parity doubling coupled with HQET [89] [91]. Radiative decays are present at the expected rate. One possible exception is the small branching ratio's reported in B decays by Belle. This has led Browder *et al.* to propose that these states are a mixture of $c\bar{s}$ and four-quark states [109]. Occam's Razor would imply that more complicated explanations are not necessary. However, more experimental information coupled with theoretical ideas will ultimately settle the issue.

9 Conclusions

Heavy quark decays is a huge field and I could only supply a short survey here, with many interesting results unfortunately omitted. Finding the effects of new physics as well as determining CKM parameters often requires the judicious use of theories and models. Theories should be used when available. Models can be useful and can give us insight into the basic physics. Models, however, when used quantitatively must be checked by comparing with similar processes in order that we can ascertain the errors due to their particular inherent assumptions. These considerations have led me to extract conservative values for $|V_{cb}| = (46.2 \pm 1.2_{exp} \pm 2.3_{thy}) \times 10^{-3}$ and $|V_{ub}| = (3.90 \pm_{exp} 0.16 \pm_{thy} 0.53) \times 10^{-3}$. These values are then used to fit for CKM parameters in the Standard Model and the allowed region can be compared with measurements of CP violation in $B^0 \rightarrow J/\psi K_s$, for example; that was done by Yamamoto at this conference [2].

Rare decays, first seen in the exclusive channel $B \rightarrow K^* \gamma$ and the inclusive channel $b \rightarrow s\gamma$ by CLEO have now been seen in $b \rightarrow s\ell^+\ell^-$ and in $B \rightarrow K\ell^+\ell^-$ by Belle, and in $B \rightarrow K^*\ell^+\ell^-$ by BaBar and Belle. These channels can show the effects of new physics when sufficient statistics are accumulated. The polarization in the K^* mode is especially important to study. Rare two-body hadronic decays are becoming precisely measured in many channels. Analysis of these decays is becoming more and more interesting.

There have been many surprises in the field of heavy quark physics. The b lifetime was predicted as being very short, below 10^{-14} s. $B^0 - \bar{B}^0$ mixing was supposed to be

too small to observe. The excited D_{sJ} states, were “known to be” wide.

If anything is predictable in this field it is that we expect surprises. Thus, finding the effects of New Physics will not be a great surprise, we expect to do it! What is not known is the kind of New Physics we will see.

This work was supported by the U. S. National Science Foundation. Many people helped by providing me with data and discussions. I am grateful to them all, although it should be clear that inclusion in this list does not mean they necessarily agree with my arguments. I thank: M. Artuso, W. Bardeen, T. Barnes, M. Beneke, M. Bona, J. Butler, K. Ecklund, E. Eichten, L. Gibbons, C. Hill, A. Kronfeld, U. Langenegger, Z. Ligeti, H. Lipkin, M. Mangano, M. Neubert, P. Roudeau, J. Rosner, N. Uraltsev, J. Urheim, M. Wise and J. C. Wang.

References

1. J. L. Rosner, Am. J. Phys. **71**, (2003) 302 [hep-ph/0206176].
2. H. Yamamoto, “Experimental Results on CP Violation,” in these proceedings.
3. T. Mannel, “Flavour physics and CP violation (theory),” in these proceedings.
4. See http://lepbosc.web.cern.ch/LEPBOSC/lifetimes/leplife_page2.html#Av .
5. D. Pedrini, in these proceedings.
6. L. Wolfenstein, Phys. Rev. Lett. **51**, (1983) 1945.
7. R. Aleksan *et al.*, Phys. Rev. Lett. **73**, (1994) 18; J. P. Silva and L. Wolfenstein, Phys. Rev. D**55** (1997) 5331.
8. <http://www.slac.stanford.edu/xorg/hfag/semi/summer03-eps/summer03.shtml>
9. N. Isgur and M. B. Wise, Phys. Lett. **B232** (1989) 113; *ibid* **B237** (1990) 527.
10. M. Luke, Phys. Lett. **B252** (1990) 447.
11. I. Caprini *et al.*, Nucl. Phys. **B530** (1998) 153.
12. M. Artuso and E. Barberio [hep-ph/0205163].
13. N. Uraltsev, in “Heavy Flavour Physics: A Probe of Nature’s Grand Design,” Proc. Intern. School of Physics, Varenna, Italy, ed. I. Bigi and L. Moroni, (IOS Press, Amsterdam, 1998) p.329 [hep-ph/9804275].
14. I. I. Bigi, [hep-ph/9612293].
15. A. H. Mahmood *et al.* (CLEO), Phys. Rev. D**67** (2003) 072001 [hep-ex/0212051].
16. C. W. Bauer *et al.*, Phys. Rev. D**67**, (2003) 054012 [hep-ph/0210027].
17. B. Aubert *et al.* (BaBar) [hep-ex/0307046].
18. M. Battaglia *et al.* DELPHI 2003-028 CONF 648 (2003).
19. A. S. Kronfeld [hep-ph/0010074].
20. P. Ball and R. Zwicky, JHEP, **0110**, (2001) 19.
21. S. B. Athar *et al.* (CLEO) [hep-ex/0304019].
22. B. Aubert *et al.* (BaBar) [hep-ex/0301001].
23. M. Luke, [hep-ph/0307378].
24. A. K. Leibovich *et al.* Phys. Lett. **B539** (2002) 242. This can also happen for neutral B mesons.
25. F. De Fazio and M. Neubert, JHEP **06** (1999) 017.
26. M. Neubert, JHEP **0007** (2000) 022 [hep-ph/0006068].
27. R. Barate *et al.* (ALEPH), Eur. Phys. J. **C6**, (1999) 555; P. Abreu *et al.* (DELPHI), Phys. Lett. **B478**, (2000) 14; M. Acciari *et al.* L3, Phys. Lett. **B36**, (1998) 173.
28. See [hep-ex/0009052].

29. A. Bornheim *et al.*, Phys. Rev. D**61**, (2002) 231803.

30. B. Aubert *et al.*, Phys. Rev. Lett. **88**, (2002) 231803.

31. See talk by Schwanda in these proceedings.

32. C. W. Bauer *et al.*, [hep-ph/0205150].

33. K. Hagiwara *et al.* (PDG), Phys. Rev. D**66**, (2002) 010001.

34. C. Cartaro, in these proceedings.

35. http://www.slac.stanford.edu/xorg/hfag/osc/aachen_2003/index.html#plot3.

36. H. Wittig in these proceedings.

37. S. Aoki *et al.* (JLQCD), [hep-ph/0307039].

38. S. D'Auria, in these proceedings.

39. H. Nelson, [hep-ex/9908021]; A. Falk *et al.*, Phys. Rev. D**65**, (2002) 054034.

40. R. Godang *et al.* (CLEO), Phys. Rev. Lett. **84**, (2000) 5038; E. Aitala *et al.* (E791), Phys. Rev. Lett. **77**, (1996) 2384; *ibid* **83**, (1999) 32; J. Link *et al.* (FOCUS), Phys. Lett. B**485**, (2000) 62; B. Aubert *et al.* (BaBar), [hep-ex/0306003]; M. Grothe, [hep-ex/0301011].

41. S. Stone, [hep-ph/0111313].

42. M. E. Peskin, [hep-ph/0002041].

43. J. C. Wang [hep-ex/0207009]; see also <http://www-btev.fnal.gov/>.

44. F. Muheim [hep-ex/0012059]; see also <http://lhcb.web.cern.ch/lhcb/>.

45. M. Ciuchini *et al.*, [hep-ph/0307195]; M. Battaglia *et al.*, [hep-ph/0304132]; M. Bargiotti *et al.*, [hep-ph/0001293]; S. Mele [hep-ph/0103040].

46. A. Hocker *et al.*, Eur.Phys. J. C**21** (2001), 225 [hep-ph/0104062].

47. <http://ckmfitter.in2p3.fr/>.

48. G. P. Dubois-Felsmann *et al.*, [hep-ph/0308262]; M. H. Schune and S. Plaszczynski [hep-ph/9911280].

49. A. Ali *et al.*, [hep-ph/9910221].

50. S. Chen *et al.* (CLEO), Phys. Rev. Lett. **87**, (2001) 251807; M. S. Alam *et al.* (CLEO), Phys. Rev. Lett. **74**, (1995) 2885.

51. R. Barate *et al.* (ALEPH), Phys. Lett. B**429**, (1998) 169; B. Aubert *et al.* (BaBar), [hep-ex/0207074], *ibid* [hep-ex/0207076]; K. Abe *et al.* (Belle), Phys. Lett. B**511**, (2001) 151.

52. C. Greub in these proceedings.

53. A. Ali *et al.*, Phys. Rev. D**66**, (2002) 034002.

54. K. Abe *et al.* (Belle), Phys. Rev. Lett. **88**, (2002) 021801.

55. A. Ryd, in these proceedings.

56. A. Ishikawa *et al.* (Belle), [hep-ex/0308044]; here they also quote an improved number on $B \rightarrow K\ell^+\ell^-$.

57. J. Kaneko *et al.* (Belle), Phys. Rev. Lett. **90**, (2003) 021801.

58. A. Ahmed *et al.* (CLEO), Phys. Rev. D**66** (2002) 031101; T. Coan *et al.* (CLEO) Phys. Rev. Lett. **88**, (2002) 062001.

59. K. Abe *et al.* (Belle), Phys. Rev. Lett. **88**, (2002) 052002.

60. B. Aubert *et al.* (BaBar), [hep-ex/0207092].

61. P. Krokovny *et al.* (Belle), Phys. Rev. Lett. **89**, (2002) 231804.

62. B. Aubert *et al.* (BaBar) [hep-ex/0207053].

63. J. Rosner, [hep-ph/0304200] and references contained therein; R. Fleischer, [hep-ph/9904313].

64. M. Beneke *et al.*, Nucl. Phys. B**606**, (2001) 245.

65. J. D. Bjorken, Nucl. Phys. Proc. Suppl. **11**, (1989) 325; M. Bauer *et al.*, Z. Phys. C**34**, (1987) 103.

66. D. Bortoletto and S. Stone, Phys. Rev. Lett. **65**, (1990) 2951.

67. Private communication from Karl Ecklund.

68. A. Bornheim *et al.* (CLEO), [hep-ex/0302026]; B. Aubert *et al.* (BaBar), [hep-ex/0308028]; B. Aubert *et al.* (BaBar), Phys. Rev. Lett. **89**, (2002) 281802; B. C. K. Casey *et al.* (Belle), [hep-ex/0207090]; L. Piilonen (Belle), in these proceedings; B. Aubert *et al.* (BaBar), [hep-ex/0308012].

69. A. Bornheim *et al.*, Phys. Rev. D **68**, (2003) 052002.

70. J. Ocariz, in these proceedings.

71. L. Piilonen, in these proceedings.

72. J. Fry at Lepton Photon 2003, Fermilab, Aug. 2003.

73. A. J. Buras *et al.*, [hep-ph/0309012].

74. Private communication from G. Buchalla.

75. W. S. Hou, in these proceedings; C.-K. Chua *et al.*, Mod. Phys. Lett. A**18**, (2003) 1763.

76. M. Moinester (Selex), [hep-ex/0212029].

77. S. K. Choi *et al.* (Belle), Phys. Rev. Lett. **89**, (2002) 102001; K. Abe *et al.* (Belle), Phys. Rev. Lett. **89**, (2002) 142001; G. Wagner (BaBar), [hep-ex/0305083]; J. Ernst *et al.* (CLEO) [hep-ex/0306060].

78. S.E. Csorna *et al.*(CLEO), [hep-ex/0207060].

79. K. Abe *et al.* (Belle), [hep-ex/0307021].

80. A. DeRujula *et al.*, Phys. Rev. Lett. **37**, (1976) 785; S. Godfrey and N. Isgur, Phys. Rev. D**32**, (1985) 189; N. Isgur and M. B. Wise, Phys. Rev. Lett. **66**, (1991) 1130; S. Godfrey and R. Kokoski, Phys. Rev. D**43**, (1991) 1679; M. Di Pierro and E. Eichten, Phys. Rev. D**64**, (2001) 114004.

81. BaBar Collaboration, B. Aubert *et al.*, Phys. Rev. Lett. **90**, (2003) 242001.

82. Fayyazuddin and Riazuddin, Phys. Rev. D**48**, (2001) 2224; reminder in [hep-ph/0309283].

83. A. Deandrea *et al.*, Phys. Lett. B**502**, (2001) 79; reminder in [hep-ph/0307069].

84. T. Barnes, F. E. Close and H. J. Lipkin, [hep-ph/0305025].

85. A. P. Szczepaniak, Phys. Lett. B**567**, (2003) 23.

86. E. van Beveren and G. Rupp, [hep-ph/0305035].

87. R. N. Cahn and J. D. Jackson, [hep-ph/0305012].

88. H. Y. Cheng and W. S. Hou, Phys. Lett. B**566**, (2003); R. Terasaki, Phys. Rev. D**68**, (2003) 011501; S. Nussinov, [hep-ph/0306187].

89. W. A. Bardeen, E. J. Eichten, and C. T. Hill, [hep-ph/0305049], based on W. A. Bardeen, and C. T. Hill, Phys. Rev. D**49**, (1994) 409.

90. P. Cho and M. B. Wise, Phys. Rev. D **49**, (1994) 6228.

91. M. A. Nowak *et al.*, [hep-ph/0307102], based on M. A. Nowak, *et al.*, Phys. Rev. D**48**, (1993) 4370.

92. D. Besson (*et al.*) (CLEO), Phys. Rev. D**68**, (2003) 032002 [hep-ex/0305100].

93. R. Seuster in these proceedings.

94. F. Porter in these proceedings.

95. M. Shapiro, "Search for Additional Decay Modes of and Partners to the $D_{sJ}^+(2317)$," FPCP, June 2003, Paris, France.

96. S. Stone and J. Urheim [hep-ph/0308166].

97. H. Lipkin, Phys. Lett. B**515**, (2001) 81.

98. P. Krokovny *et al.* (Belle), [hep-ex/0308019].

99. K. Abe *et al.* (Belle), [hep-ex/0307052].

100. C. H. Chen and H. Li, [hep-ph/0307075].

101. A. Datta and P. J. O'Donnell, [hep-ph/0307106].

102. S. Godfrey, Phys. Lett. B**568**, (2003) 254.

103. P. Colangelo and F. De Fazio, [hep-ph/0305140].

104. A. Dougall *et al.*, Phys. Lett. B**569**, (2003) 41.

105. G. Bali, [hep-ph/0305209].

106. M. Sadzikowski, [hep-ph/0307084].

107. Y. B. Dai *et al.*, [hep-ph/0306274].

108. W. Lucha and F. Schöberl, [hep-ph/0309341].

109. T. Browder *et al.*, [hep-ph/0307054].

